Proc. Natl. Acad. Sci. USA
Vol. 95, pp. 4362–4367, April 1998
Cell Biology

Dynamics of contacts between lamellae of fibroblasts: Essential role of the actin cytoskeleton

(contractility/myosin/adherens junctions/β-catenin/neoplastic transformation)

N. A. GLOUSHANKOVA*, M. F. KRENDEL†‡, N. O. ALIEVA*§, E. M. BONDER†‡¶, H. H. FEDER†, J. M. VASILIEV*§, AND I. M. GELFAND§‖

‡Program in Cellular and Molecular Biodynamics and †Department of Biological Sciences, Rutgers University, Newark, NJ 07102; ‖Department of Mathematics, Rutgers University, Piscataway, NJ 08854; and *Oncological Scientific Center of Russia and §Belozersky Institute of Physico-Chemical Biology, Moscow State University, Moscow 115522, Russia

Contributed by I. M. Gelfand, January 16, 1997

ABSTRACT **We investigated actin cytoskeletal and adhesion molecule dynamics during collisions of leading lamellae of nontransformed and oncogene-transformed fibroblasts. By using real-time video microscopy, it was found that during lamellar collision there was considerable overlapping of leading lamellae followed by subsequent retraction. Overlapping of nontransformed fibroblasts was accompanied by formation of β-catenin-positive contact structures organized into strands oriented parallel to the long axis of the cell that were associated with bundles of actin filaments. Maintenance of such cell–cell contact structures critically depended on the contractility of actin cytoskeleton, as inhibition of contractility with serum-free medium or 2,3-butanedione 2-monoxime (BDM) resulted in loss of strand formation. Strand formation was recovered when cells in serum-free medium were incubated with the microtubule inhibitor nocodazole, which is known to increase contractility. Oncogene-transformed fibroblasts reacted to collisions with responses similar to nontransformed fibroblasts but did not develop well-organized cell–cell contacts. A model is presented to describe how differences in the organization of the actin cytoskeleton could account for the structurally distinct responses to cell–cell contact by polarized fibroblastic cells versus nonpolarized epithelial cells.**

The ability of cultured cells to form multicellular tissue-like structures, such as epithelial sheets or monolayered streams of fibroblasts, relies upon formation of appropriate cell–cell adhesion and structural organization of the cytoskeleton. When a cell first makes contact with a neighboring cell it undergoes contact inhibition of movement, preventing continued forward translocation across the surface of its neighbor (1).

Previously, we reported that epitheliocytes and their *ras*-transformed descendants exhibited distinct responses to cell–cell contact as judged by formation of adherens junctions, motility of membrane-associated proteins, and organization of the actin cytoskeleton (2). We now set out to determine whether the observed responses to cell–cell collision were related to differences in the structural organization of the two cell lines (nonpolarized versus polarized morphology) or to transformation with a mutant *ras* oncogene. In the context of these studies, polarized and nonpolarized refers to the spatial organization of lamellar pseudopodial activity and not to apical versus baso-lateral polarization. Cell–cell collisions in three fibroblast cell lines, nontransformed human and rat fibroblasts and *ras*-transformed descendants of the rat fibroblast line, were examined with respect to organization of the actin cytoskeleton, motility of beads attached to the cell surface, and formation of adherens-type junctions. In all cell lines examined, collisions resulted in significant overlapping of lamellae, formation of transient cell–cell contacts aligned along the axis of the cell followed by retraction of the overlapping lamellae, development of new lateral lamellae, and a change in the direction of cell movement. Combined with our earlier studies (2), it is suggested that regardless of a cell's origin (fibroblastic or epithelial), the dynamics of cell–cell contact and contact inhibition of movement are intimately linked to the organization of the cell's cytoskeleton.

MATERIALS AND METHODS

Cell Culture and Light Microscopy. AG-1523 human diploid fibroblasts (kindly provided by C. Heckman, Bowling Green State University), Rat-1 fibroblasts (3), and Rat-1/*ras* (4) fibroblasts were cultured in DMEM supplemented with 10% fetal calf serum and antibiotics at 37°C and 5% CO_2. For video observation, cells were grown on glass coverslips, and cell monolayers were wounded and allowed to recover for 3–4 hr prior to observation. To inhibit contractility, monolayers of Rat-1 cells were wounded and upon initiation of cell–cell contact they were treated with serum-free DMEM or 25 mM 2,3-butanedione 2-monoxime (BDM) in DMEM containing serum. In some experiments, incubation with serum-free DMEM was followed by 30-min treatment with nocodazole (10 μg/ml) in serum-free DMEM. Differential interference contrast microscopy of live cells and analysis of bead motility were performed as described (2).

Immunofluorescence Staining and Confocal Microscopy. For simultaneous localization of actin and β-catenin, cells were rinsed with PBS, fixed in PBS containing 3.7% formaldehyde, permeabilized for 3 min with 1% Triton X-100 in PBS, and stained with rhodamine-phallodin to label actin filaments and mAbs against β-catenin (Transduction Laboratories, Lexington, KY) followed by fluorescein isothiocyanate-labeled goat anti-mouse secondary antibodies. For actin and myosin II labeling, cells were permeabilized and subsequently fixed as described (5). Fixed cells were incubated with rhodamine-phalloidin and polyclonal antibodies against nonmuscle myosin II (BioMedical Technologies, Stoughton, MA). Antimyosin antibodies were visualized by using Oregon Green-conjugated goat anti-rabbit secondary antibodies (Molecular Probes). Identical results for myosin localization were obtained when cells were simultaneously fixed and permeabilized prior to

The publication costs of this article were defrayed in part by page charge payment. This article must therefore be hereby marked "*advertisement*" in accordance with 18 U.S.C. §1734 solely to indicate this fact.

Abbreviation: BDM, 2,3-butanedione 2-monoxime.

¶To whom reprint requests should be addressed at: Program in Cellular and Molecular Biodynamics, Department of Biological Sciences, Rutgers University, 101 Warren Street, Newark, NJ 07102. e-mail: ebonder@andromeda.rutgers.edu.

staining. Fluorescence images were collected by using a Bio-Rad MRC 1024 laser scanning confocal microscope equipped with Nikon optics.

RESULTS

Analysis of Cell–Cell Collisions. AG fibroblasts possessed wide lamellae limited to the front end of the elongated cell body. Rat-1 fibroblasts had flat polygonal cell body and narrow lamellae. Rat-1/*ras* fibroblasts were highly elongated, the central part of the cell body was not attached to the substratum, and the relatively small leading lamellae had numerous ruffles. "Head-on collisions" by the active leading lamellae of cells migrating into wounds within monolayers exhibited the following common series of changes for all three cell lines.

Overlapping of lamellae. After initial cell–cell contact, the leading edge of one lamella continued to move across the surface of the other cell's lamella (Fig. 1 *A* and *C*). Occasionally, the lower lamella continued to move forward along the coverslip under the upper lamella.

Retraction. After establishing an overlap, the upper lamella retracted from the surface of the lower cell. Retraction did not begin simultaneously across the entire edge of the cell. Most often there was a gradual narrowing of the lamella, resulting initially in a serrated edge that with continued retraction led to formation of microspike-like projections linking the retracting lamella to the surface of the underlying cell.

Formation of a new lamella. During retraction, a new lamella formed by expansion from a segment of the lamella that was still adherent to the glass substratum and not involved in cell–cell contact (Fig. 1 *B* and *D*). Whenever the entire lamella was involved in overlapping, a new lamella developed along the lateral edge of the cell.

Directional change. Retraction of the overlapping lamella and expansion of a new lateral lamella led to the shift in the direction of the cell movement and migration of colliding cells away from each other.

Although the described sequence of events following cell–cell collisions was similar in all three lines of fibroblasts, the duration of individual stages and extent of lamellar overlapping were different for each cell line. The maximal length of measured overlap, that is the distance between the edges of overlapping lamellae, was ≈9–16 μm for AG fibroblasts and 5–10 μm for Rat-1 fibroblasts. The degree of overlap was smaller in Rat-1/*ras* fibroblasts at ≈3–5 μm. The duration of the overlapping lamella stage of the interaction was variable, ranging from 10–15 min for AG, 20–40 min for Rat-1, and only 2–5 min for Rat-1/*ras* cells.

The rate of centripetal movement of Con A-coated beads attached to the free leading edges of the fibroblasts moving into the wound was similar in AG and Rat-1 cell lines and significantly higher in Rat-1/*ras* cells (Table 1). Neither the direction nor the rate of bead movement changed significantly when attached to the surface of overlapping lamellae in colliding cells (Table 1).

Organization of the Actin Cytoskeleton and β-Catenin. AG fibroblasts contained a meshwork of thin actin bundles in relatively wide active lamellae and thick, straight actin stress fibers within the central part of the cell were, typically, aligned with the long axis (Fig. 2 *A*, *B*, *D*, and *G*). Indirect immunofluorescence staining for myosin II revealed that the cell body and proximal part of the lamella were enriched in myosin II, whereas the distal one-third to one-half of the lamella was largely devoid of myosin II (see Fig. 2 *A* and *B*). Myosin II appeared to be associated both with stress fibers and a fine meshwork of filamentous actin. There was no pronounced change in the organization of actin filaments during lamellar overlapping. Upon retraction, actin filaments started to become linearly organized within the serrated retracting edge, eventually leading to formation of thin bundles of actin filaments projecting radially away from the cell edge (Fig. 2*G*). The overlapping lamellae and the distal nonoverlapping lamellae were essentially free of myosin II (Fig. 2*A*), although

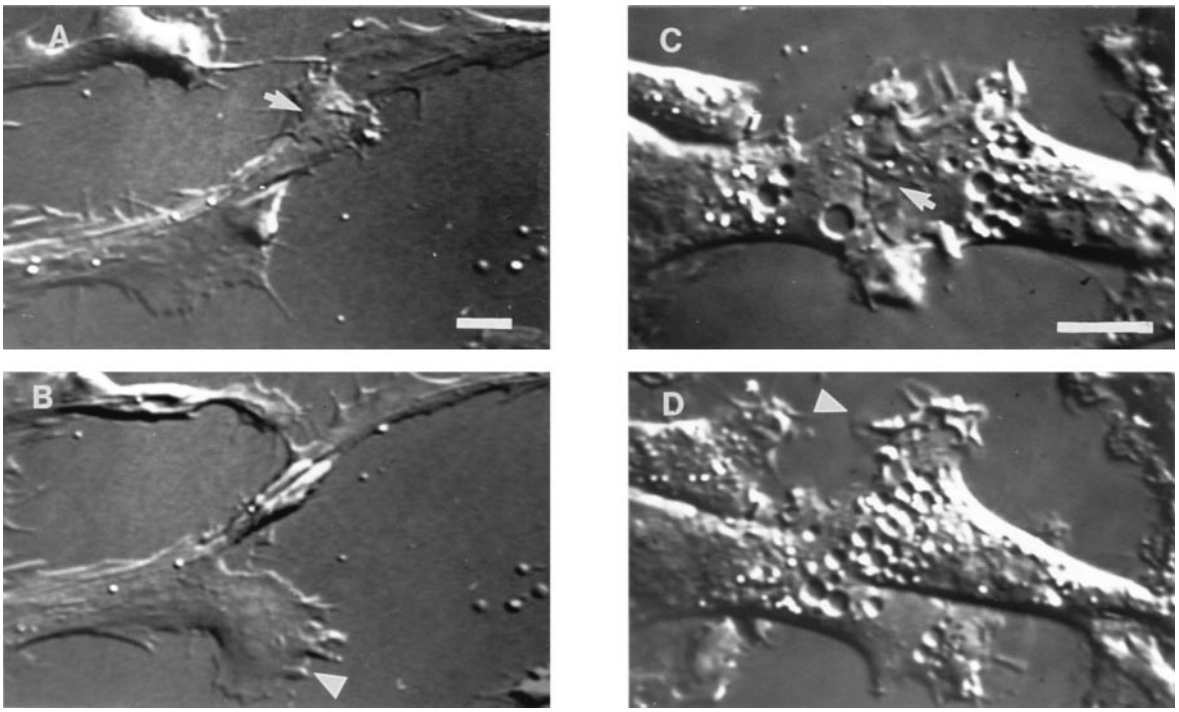

FIG. 1. Observation of cell–cell contact between migrating fibroblasts. Video-differential interference contrast micrographs of AG (*A* and *B*) and Rat-1/*ras* (*C* and *D*) fibroblasts. During early stages of cell–cell contact (*A* and *C*) the leading edges of migrating cells produced overlapping lamellae (arrows). Sometime later, the overlapping lamellae retracted and a new lamella was extended from a free cell edge (*B* and *D*; see arrowheads). Protrusion of a new lamella led to a change in direction of cell movement (*B* and *D*), so that eventually cells moved away from each other. Time interval between *A* and *B* is 20 min, and between *C* and *D* is 12 min. (Bar = 10 μm.)

Table 1. Rates of centripetal movement (μm/min) of surface attached beads at the free cell edges and on overlapping lamellae after cell–cell collisions

Cell line	Free edge	Overlapping lamellae
AG	0.99 ± 0.09	0.99 ± 0.14
Rat-1	0.83 ± 0.10	0.94 ± 0.25
Rat-1/*ras*	1.54 ± 0.23	1.73 ± 0.24

the myosin-free area became smaller as retraction proceeded (see Fig. 2*B*).

Rat-1 fibroblasts had an extensive lattice-like network of myosin II containing stress fibers spread throughout the cell body (Fig. 2*C*). The active lamellae of Rat-1 fibroblasts possessed a meshwork of actin filaments and no detectable myosin II. There was no recognizable change to the overall organization of actin filaments or myosin II within the overlapping lamellae and subsequent retraction occurred essentially as described for AG fibroblasts.

Rat-1/*ras* cells contained a small number of straight, thin bundles of actin filaments that were oriented with the long axis of the cell. Myosin II was evenly distributed throughout the cell body and was absent from the actin-rich ruffles at the cell edge. Cell–cell collisions had little effect on the organization of actin and myosin II, although areas of cell–cell contacts usually contained fewer actin-filled ruffles.

In individual AG and Rat-1 cells, β-catenin, a characteristic component of adherens junctions, was diffusely localized across the entire surface of the cell. At early stages of cell–cell contact, there was a spotted enrichment of β-catenin within the overlapping lamellae (Fig. 2*E*). In later stages of overlap, anti-β-catenin labeling occurred along a serrated edge and in long strands within the overlapping lamellae (Fig. 2 *H* and *K*). The strands were oriented perpendicular to the edge of the

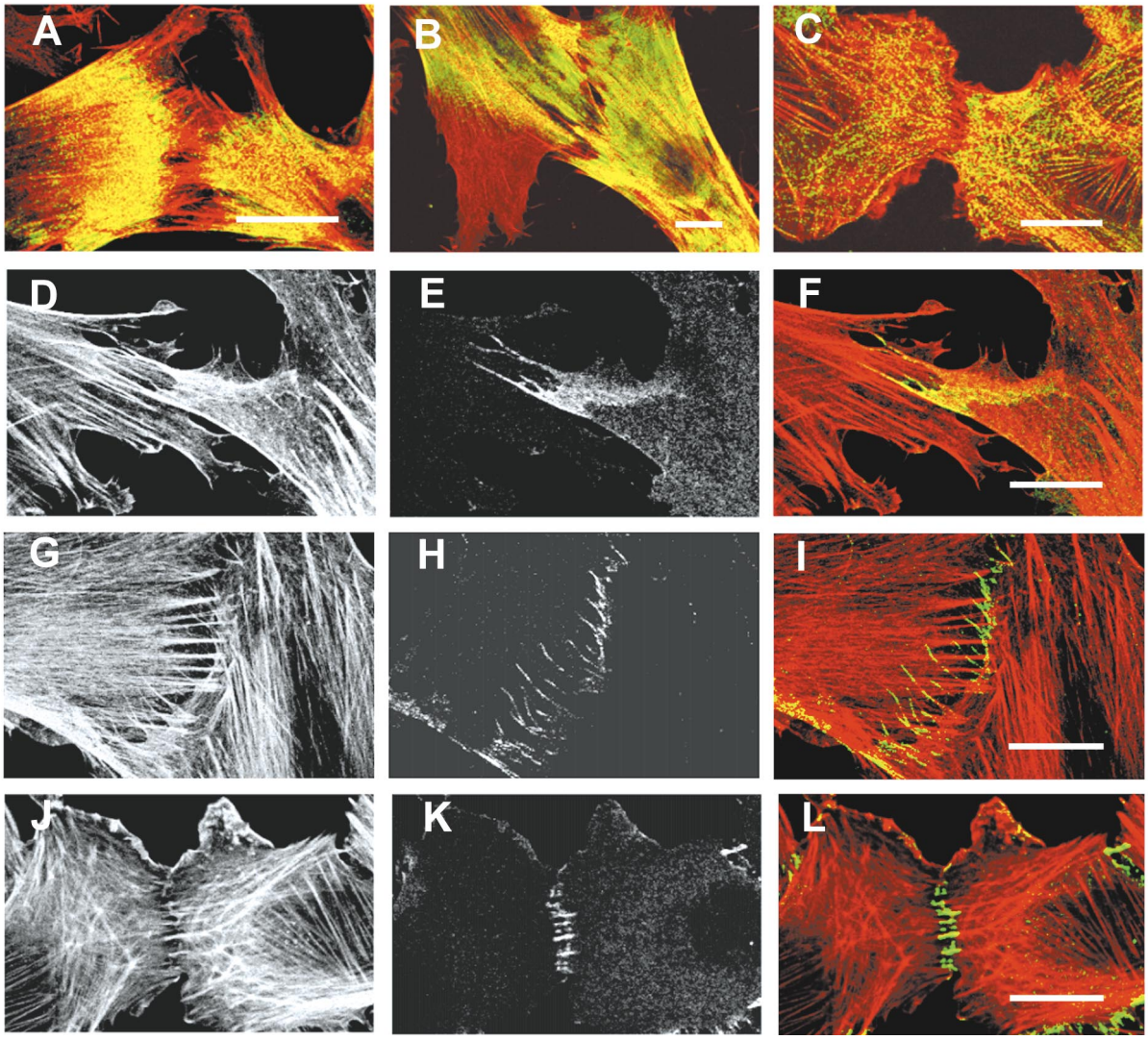

FIG. 2. Immunofluorescence localization of actin, myosin II, and β-catenin in contacting fibroblasts. (*A–C*) Contacting fibroblasts of cell lines AG (*A* and *B*) and Rat-1 (*C*) were fixed and double-labeled for actin (red) and myosin II (green). Areas in yellow indicate regions where actin and myosin staining coincided. Myosin II is concentrated in the proximal region of lamellae and absent from the distal regions creating a myosin-free gap between contacting cells (*A* and *C*). Retraction of overlapping lamellae results in a narrowing of the myosin-free area (*B*). Note the large actin-rich lamella lacking myosin extending laterally away from the site of cell–cell contact (*B*). (*D–L*) Contacting AG (*D–I*) and Rat-1 (*J–L*) fibroblasts were fixed and double-labeled for actin filaments (*D*, *G*, and *J*) and β-catenin (*E*, *H*, and *K*). Actin and β-catenin images were superimposed to create color representations of actin and β-catenin distribution where actin is shown in red, β-catenin in green, and areas where the two coincide are indicated in yellow (*F*, *I*, and *L*). Early stages of contact between AG cells showed enrichment of β-catenin in overlapping lamella (*E* and *F*). At later stages of AG cell–cell contact, β-catenin was located in strands within the contact area (*H*) that colocalized with the ends of thin actin filament bundles (*I*). In contacting Rat-1 cells, transverse β-catenin strands in the contact area are attached to the ends of actin filament bundles (*J*, *K*, and *L*). (Bar = 20 μm.)

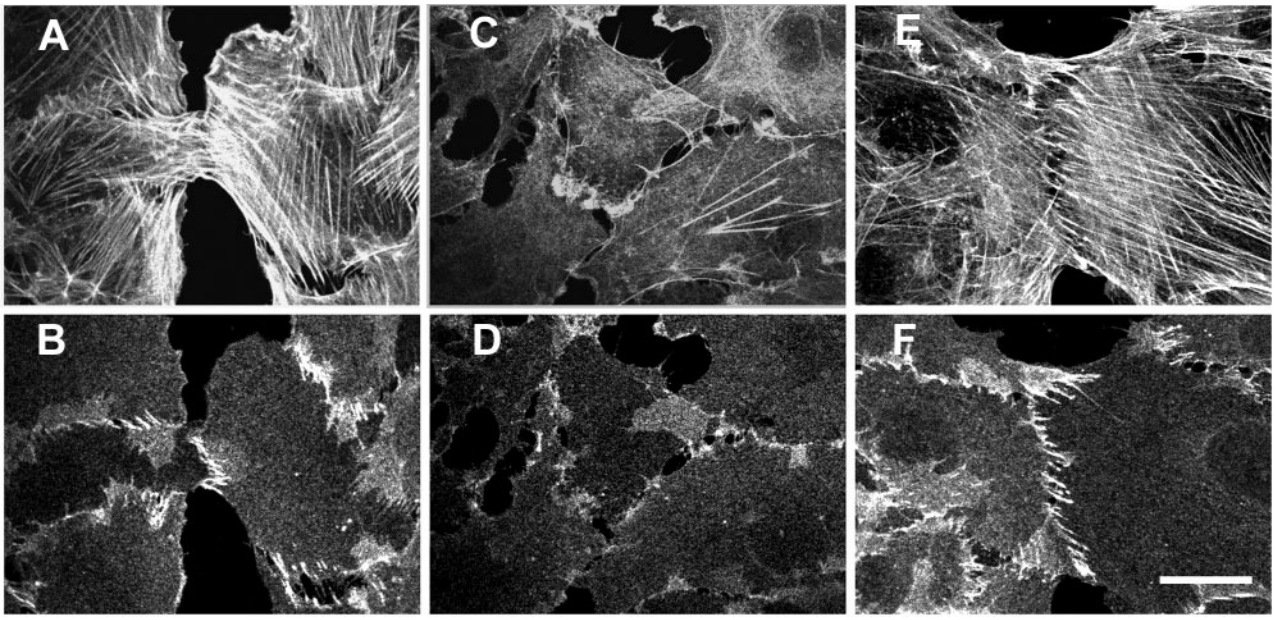

FIG. 3. Effect of inhibition of myosin-mediated contractility on adherens junction organization. Contacting Rat-1 cells were incubated in serum supplemented DMEM without any additives (control, *A* and *B*), DMEM with serum and the myosin inhibitor BDM (25 mM) for 40 min (*C* and *D*), or DMEM with serum and 25 mM BDM for 40 min followed by washout of BDM for 1 hr (*E* and *F*). Cells were double-labeled for actin (*A*, *C*, and *E*) and β-catenin (*B*, *D*, and *F*). Treatment with BDM resulted in disassembly of the majority of actin filament bundles (compare *A* and *C*) and loss of transverse strands of β-catenin (compare *B* and *D*). Removal of BDM led to complete restoration of actin filament bundles and cell–cell contact organization (*E* and *F*). (Bar = 20 μm.)

cell, and confocal microscopy of cells double labeled for actin filaments and β-catenin established the superposition of the β-catenin strands with the ends of thin bundles of actin filaments (Fig. 2 *I* and *L*). The bundles of actin filaments associated with the β-catenin strands were somewhat thinner than stress fibers (Fig. 2*G*), did not exhibit punctate myosin II staining, and their ends did not terminate in paxillin stained focal contacts (data not shown). Rat-1/*ras* cells exhibited mostly diffuse distribution of β-catenin with occasional "spots" of bright staining and β-catenin containing strands were not observed (data not shown).

Effect of Myosin-Based Contractility on Cell–Cell Contact Formation. Given the spatial and temporal correlation between the reorganization of β-catenin localization from diffuse lamellar enrichment to elongate strands with the formation of actin filament bundles and lamellar retraction, we suggest that strand formation was driven by myosin-dependent contraction. To test this hypothesis, Rat-1 cells were incubated either in serum-free DMEM or DMEM containing the myosin inhibitor BDM (6, 7) to inhibit myosin-based contractile activity. Both treatments resulted in disassembly of actin stress fibers and formation of actin-rich ruffles at free cell edges (Figs. 3*C* and 4*A*). Additionally, β-catenin strands disappeared and occasionally narrow ribbons of contiguous β-catenin staining spots were observed (Figs. 3*D* and 4*B*). There also appeared to be a general reduction in the amount of β-catenin associated with the overlapping region. Exposing cells to lower doses of BDM or shorter incubation times with serum-free medium resulted in partial disassembly of the actin bundles within the lamella. In such cells, transverse β-catenin strands were associated with the ends of the actin filament bundles, whereas the majority of the cell–cell contacts had a spotted ribbon appearance (data not shown). To reverse the effect of serum starvation, cells were exposed to the microtubule-depolymerizing drug nocodazole which increases the contractility of the actin cytoskeleton (8, 9). Nocodazole treatment resulted in the reappearance of

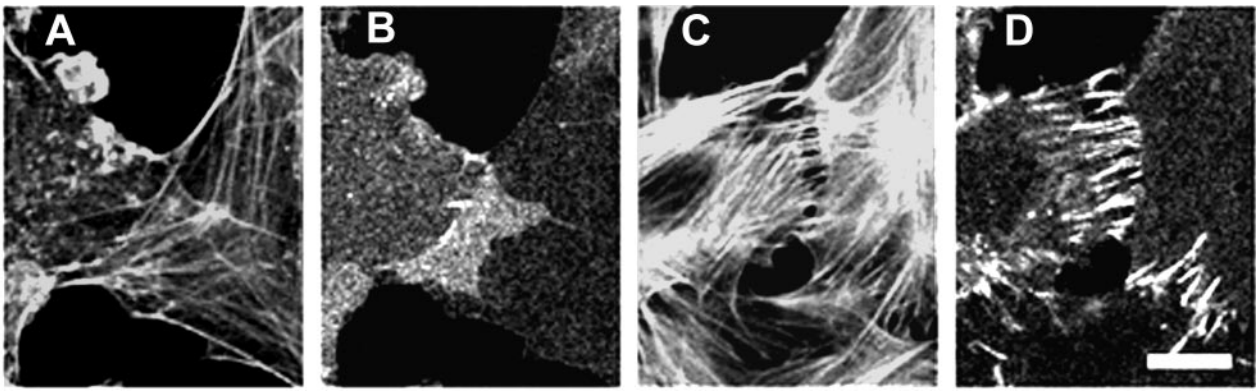

FIG. 4. Effect of increased contractility on organization of cell–cell contacts in serum-starved Rat-1 fibroblasts. Contacting Rat-1 fibroblasts were incubated in serum-free medium for 40 min and then treated with serum-free medium containing nocodazole. Cells treated with serum-free medium contained only a small number of thin actin filament bundles (*A*) and β-catenin was mostly diffusely distributed throughout the cell (*B*). The elevated level of β-catenin staining (see *B*, center) in some parts of serum deprived cells appears to simply result from superposition of two overlapping lamellae. Activation of contractility with nocodazole led to assembly of numerous actin bundles (*C*) and formation of transverse β-catenin strands at sites of cell–cell contact (*D*). (Bar = 10 μm.)

bundles of actin filaments (Fig. 4*C*) and long, transverse strands containing β-catenin (Fig. 4*D*).

DISCUSSION

We found that homologous cell–cell collisions between nontransformed and oncogene-transformed fibroblasts (cells with polarized pseudopodial activity) resulted in qualitatively similar sequences of reactions that included significant overlapping of lamellae followed by lamellar retraction and development of new lateral lamellae. Formation of overlapping lamellae by fibroblasts was not accompanied by any detectable change either in the number and orientation of actin bundles or in the rate and direction of movement of beads attached to the top surface of an overlapping lamella. Contact inhibition of forward cell movement in transformed and nontransformed fibroblasts occurred only after a significant period of lamellar overlap that eventually led to redirected movement away from the point of contact. A similar response to cell–cell contact was observed for *ras*-transformed epitheliocytes that acquired fibroblast-like morphology (2). Alternatively, nontransformed discoid epitheliocytes (cells with nonpolarized pseudopodial activity) developed a small lamellar overlap, "paralysis" of the lamellar edge, and lateral expansion of the cell–cell contacts. Furthermore, beads attached to the surface of the contacting lamella started to move tangentially rather then centripetally during expansion of the contact. Taken together, these results suggested that polarized cells with fibroblastic morphology and nonpolarized discoid epitheliocytes were capable of undergoing the phenomena of contact inhibition of forward movement; however, they accomplish this task by two qualitatively different modes of action.

Role of the Actin Cytoskeleton in Determining the Response to Cell–Cell Contact. An important difference between the two cell types being studied is the organization of their actin cytoskeleton. The key differences in cytoskeletal organization are most readily observed in individual cells spread on the substrate with epithelial cells containing prominent circular, marginal actin bundles, whereas fibroblast-like cells have many straight actin bundles and no marginal bundle. We propose that these organizational differences play an important role in determining the physiological response to cell–cell contact.

In epitheliocytes, rapid formation of adherens junctions is paralleled by disassembly of the marginal bundle of actin filaments followed by formation of a marginal "arc" of actin filaments at the expanding edge of the contact. Lateral expansion of the zone of contact and paralysis of pseudopodial activity were proposed to be a consequence of tangential traction that developed along the newly reorganized marginal actin bundles (ref. 2; also see Fig. 5). Because fibroblasts do not possess a marginal bundle of actin filaments, they are not capable of producing lateral tension along actin arcs; instead, the cell is most efficient at producing tension along the long, or migratory, axis of the cell (Fig. 5). Accordingly, lamellae of fibroblasts and fibroblast-like cells developed significant overlapping after cell–cell collision and areas of lamellar overlapping expanded along the longitudinal axis of the cell. Eventually, longitudinal tension would orient actin filaments within the overlapping lamella and the lamellae would begin retraction via myosin-mediated contraction. This idea is consistent with the proposed role of myosin II in contraction of the cell body (10, 11). Thus, the observed differences in epithelial and fibroblastic cell responses to cell–cell collisions may be caused by the formation of actin cytoskeleton-dependent lateral tension in epithelial cells versus centripetal tension in fibroblasts.

Polarized and Nonpolarized Cells Form Two Different Types of Adherens Junctions upon Cell–Cell Contact. As previously described (12–14), adherens junctions form between the lamellae of contacting nontransformed fibroblasts. One may suggest that the various β-catenin containing structures we observed by immunofluorescence represent stages in the formation of cell–cell adhesion junctions. For example, β-catenin-positive spots could be formed by actin-dependent coalescence of adhesion molecules during lamellar overlapping, whereas subsequent lamellar retraction induced first the formation of a serrated β-catenin contact followed by the appearance of elongate β-catenin strands. These changes can be contrasted with nontransformed epitheliocytes where contacts formed between the lateral edges of the cell and β-catenin was localized to ribbons oriented tangentially along colliding cell edges. Fibroblasts make contacts between the lower and upper surfaces of overlapping lamellae and β-catenin-positive strands are often oriented perpendicular to the cell edge. How might the different structural orientation of adhesion contacts form during the events of cell–cell contact?

Tension developed by attached actin bundles is known to be essential for elongation of focal adhesions of fibroblasts with the substratum (7, 9, 15). It seems plausible that the direction of cellular tension may serve as the orienting force for adhesion contacts as well as focal contacts. This suggestion was supported experimentally by the observed loss of β-catenin strands when myosin contractility was inhibited and the formation of β-catenin strands when contractility was stimulated. Thus we conclude that tangential tension induces tangential orientation and elongation of cell–cell contacts in epitheliocytes (2), whereas centripetal tension in fibroblasts leads to longitudinal orientation of elongate β-catenin containing strands (Fig. 5). While emphasizing the importance of actin cytoskeletal activity in the formation of adhesion junctions, it is important to recognize that adhesion molecule expression is

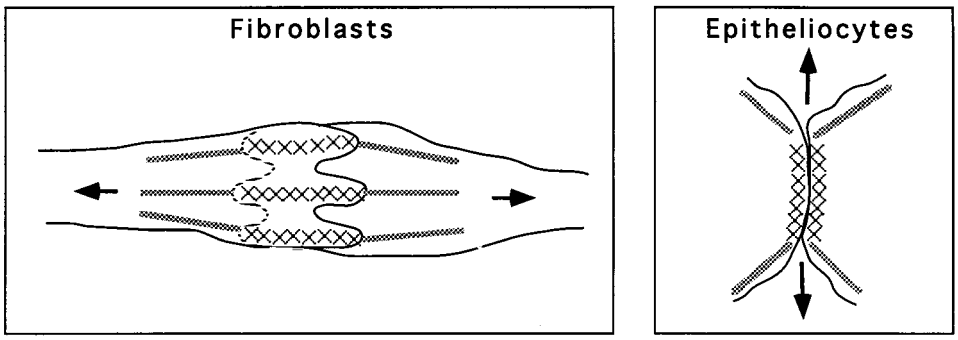

FIG. 5. Schematic representation of the two mechanisms of cell–cell contact formation. (*Left*) In fibroblasts and fibroblast-like cells cell–cell interaction results in overlapping of the lamellae of contacting cells. Centripetal tension (arrows) from acto-myosin bundles (gray lines) in the cell body leads to retraction of overlapping lamellae. As a result of retraction, cell adhesion molecules in the area of the cell–cell contact (crosses) are aligned into thin strands oriented along the cell axis. (*Right*) In epitheliocytes, cell–cell contacts expand laterally, and this expansion is likely to be driven by tension (arrows) generated along marginal actin bundles (gray lines) at the edges of the contact. Lateral, rather than centripetal, direction of tension forces also results in tangential orientation of cell adhesion molecules in epitheliocytes.

equally important in the formation of cell–cell contacts (16, 17). Although it is beyond the scope of this report, there is no doubt that understanding the complex interplay between adhesion molecule activity and the structural and functional dynamics of the actin cytoskeleton is of fundamental importance.

Nontransformed and Oncogene Transformed Fibroblasts Both Exhibit Contact Inhibition. Cultures of oncogene-transformed cells usually consist of multilayered criss-crossed cells, whereas nontransformed fibroblasts form monolayered colonies with streams of nearly parallel cells. It is often suggested that the reason for these differences is the loss of contact inhibition of movement leading to more pronounced cell overlapping after cell–cell collisions. However, in our experiments both nontransformed and *ras*-transformed fibroblasts demonstrated qualitatively similar reactions to cell–cell collisions. In both cases cell overlapping was transient and, in fact, the extent and duration of overlapping were even lower during collisions of *ras*-transformed cells than for their nontransformed ancestors. Abnormal organization of colonies of transformed fibroblasts may not be caused by the lack of contact inhibition during head-on collisions but rather by decreased attachment to the substratum and/or by weak cell–cell adhesion (18–20).

In summation, it is suggested that contact inhibition of movement of one cell over the other can be achieved through two different sets of reactions linked to actin cytoskeleton dynamics.

(*i*) Reactions characteristic of epithelial cells with nonpolarized pseudopodial activity involve significant reorganization of actin cytoskeleton leading to formation of actin bundles that participate in tangential tension production, thereby driving formation of permanent tangentially oriented cell–cell contacts (2).

(*ii*) Reactions characteristic of fibroblast-like cells with polarized pseudopodial activity involve transient overlapping of lamella followed by myosin-dependent contraction along radially positioned bundles of actin filaments that guide the formation of transient radially oriented cell–cell contacts.

This work was supported by the Gabriella and Paul Rosenbaum Foundation (to I.M.G.), a Russian Foundation of Basic Investigations Grant (to J.M.V.), and an American Heart Association, New Jersey Affiliate, grant and the Charles and Johanna Busch Memorial Fund (to E.M.B.).

1. Abercrombie, M. (1970) *In Vitro* **6,** 128–142.
2. Gloushankova, N. A., Alieva, N. A., Krendel, M. F., Bonder, E. M., Feder, H. H., Vasiliev, J. M. & Gelfand, I. M. (1997) *Proc. Natl. Acad. Sci. USA* **94,** 879–883.
3. Steinberg, B., Pollack, R., Topp, W. & Botchan, M. (1978) *Cell* **3,** 19–32.
4. Stromskaya, T. P., Grigorian, I. A., Ossovskaya, V. S., Rybalkina, E. Y., Chumakov, P. M. & Kopnin, B. P. (1995) *FEBS Lett.* **368,** 373–376.
5. Svitkina, T. M., Shevelev, A. A., Bershadsky, A. D. & Gelfand, V. I. (1984) *Eur. J. Cell Biol.* **34,** 64–74.
6. Cramer, L. P. & Mitchison, T. J. (1995) *J. Cell Biol.* **131,** 179–189.
7. Chrzanowska-Wodnicka, M. & Burridge, K. (1996) *J. Cell Biol.* **133,** 1403–1415.
8. Danovski, B. (1989) *J. Cell Sci.* **93,** 255–266.
9. Bershadsky, A., Chausovsky, A., Becker, E., Lyubimova, A. & Geiger, B. (1996) *Curr. Biol.* **6,** 1279–1289.
10. Conrad, P. A., Giuliano, K. A., Fisher, G., Collins, K., Matsudaira, P. T. & Taylor, D. L. (1993) *J. Cell Biol.* **120,** 1381–1391.
11. Mitchison, T. J. & Cramer, L. P. (1996) *Cell* **84,** 371–379.
12. Heaysman, J. E. & Pegrum, S. M. (1973) *Exp. Cell Res.* **78,** 71–78.
13. Yonemura, S., Itoh, M., Nagafuchi, A. & Tsukita, S. (1995) *J. Cell Sci.* **108,** 127–142.
14. Knudsen, K. A., Soler, A. P., Johnson, K. R. & Wheelock, M. J. (1995) *J. Cell Biol.* **130,** 67–77.
15. Vasiliev, J. M. (1985) *Biochim. Biophys. Acta* **780,** 21–65.
16. Behrens, J., Mareel, M. M., Van Roy, F. M. & Birchmeier, W. (1989) *J. Cell Biol.* **108,** 2435–2447.
17. Gumbiner, B. M. (1996) *Cell* **84,** 345–357.
18. Guelstein, V. I., Ivanova, O. Y., Margolis, L. B., Vasiliev, J. M. & Gelfand, I. M. (1973) *Proc. Natl. Acad. Sci. USA* **70,** 2011–2014.
19. Takeichi, M. (1993) *Curr. Opin. Cell Biol.* **5,** 806–811.
20. Mareel, M., Boterberg, T., Noe, V., Van Hoorde, L., Vermeulen, S., Bruyneel, E. & Bracke, M. (1997) *J. Cell Physiol.* **173,** 271–274.